Two Devices for Longitudinal Emission Tomography of the Thyroid

John W. van Giessen, Max A. Viergever, Peter P. van Rijk, and J. Georges Gerritsen

Department of Mathematics and Informatics, Delft University of Technology, 2600 AJ Delft, The Netherlands; and Institute of Nuclear Medicine, University Hospital Utrecht, 3511 GV Utrecht, The Netherlands

Two devices especially designed for tomographic thyroid imaging are compared on the basis of phantom experiments and four patient studies: a seven pinhole (7P) collimator and a time-coded aperture (TCA). The results of patient studies show that the 7P collimator may miss smaller abnormalities and is prone to incorrect positioning. The TCA reconstructions of patient data confirm the good performance observed in the phantom studies and demonstrate a high degree of lesion detectability. The TCA also provides higher efficiency and shorter imaging times than the 7P collimator. It is therefore concluded that TCA imaging is a promising alternative to multiple view pinhole imaging of the thyroid.

J Nucl Med 28:1892–1900, 1987

We have studied two devices for longitudinal emission tomography of the thyroid: a seven pinhole (7P) collimator (*1*) and a time-coded aperture (TCA) (*2*).

The 7P collimator was originally designed for myocardial tomographic imaging by Vogel et al. (*3,4*). We have optimized the reconstruction software (*5*), thereby removing the main objections against the device. Furthermore, we have redesigned the system for the needs of thyroid tomography. Geometric arguments suggest that the 7P device is more suited for thyroid imaging than for myocardial imaging (*1*).

The time-coded aperture was originally designed by Koral et al. (*6,7*). Their system was capable of producing good quality reconstructions (*8,9*), but there were difficulties in keeping the reconstruction time within reasonable limits. Resinger et al. (*9*) reported a minimum computation time of 2 hr on a commercial nuclear medicine computer system. Our reconstruction program, which takes ~11 min using a 588 kbyte memory partition of a 16 bit minicomputer, produces good quality phantom reconstructions (*2*). We improved the design of the device in several ways which have increased the sensitivity of the system and have facilitated the handling of the collimator.

The purpose of this paper is to compare the two devices on the basis of the phantom experiments described in (*1,2*) and, especially, of patient data. We recorded thyroid projections from four patients, both with the 7P collimator and with the TCA device. Of course, no statistically valid conclusions can be drawn on the grounds of only four cases. This study merely intends to give an indication of the capabilities of both devices.

Received July 18, 1986; revision accepted June 11, 1987.

For reprints contact: John W. van Giessen, Dept. of Mathematics and Informatics, Delft University of Technology, P.O. Box 356, 2600 AJ Delft, The Netherlands.

METHODS

The Two Devices and Their Environment

Both devices are designed to be mounted on a large field-of-view gamma camera (effective diameter 380 mm, intrinsic FWHM resolution 4 mm). The camera has built-in electronics that correct for nonlinearities and energy distortions (in practice, this means that there is virtually no need for a nonuniformity correction).

The preprocessing and reconstruction of the data is performed in a 588 kbyte memory partition of a 16-bit minicomputer with a (pipeline) vector processor. A video image processor linked to this system is used for display of raw data and results of the reconstruction process.

The *thyroid 7P collimator* is a modification of the 7P system that was developed for heart tomography by Vogel et al. (*3, 4*). The collimator consists of a lead pinhole plate, located at 60 mm from the camera crystal, with seven pinholes of 4 mm diameter. The center of the central pinhole is situated on the optical axis of the system (Fig. 1). The six peripheral pinholes are spaced evenly at 63.5 mm from the axis. Following i.v. injection of a suitable radionuclide (e.g., ^{123}I), this configuration records seven projected images of the radioactivity distri-

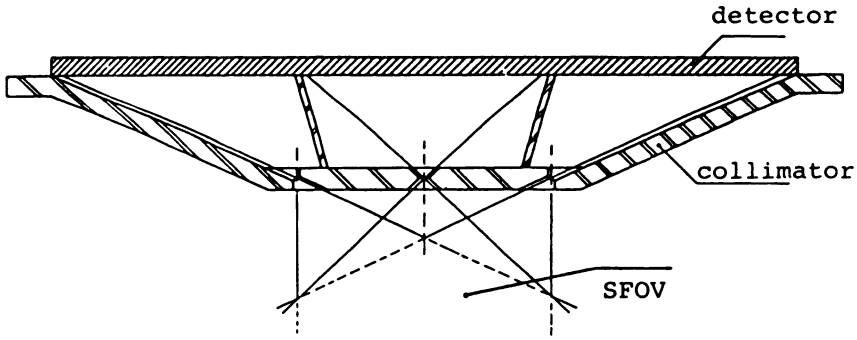

FIGURE 1
The 7P thyroid collimator. The dashed lines encompass the simultaneous field of view (SFOV).

bution in the thyroid (and its surroundings). The projections are nonoverlapping owing to lead septa placed between adjacent pinholes (Fig. 1). The pencil-shaped volume simultaneously viewed by the projection sectors through the corresponding pinholes is the reconstruction volume (Figs. 1 and 2). The camera should be positioned so that the thyroid falls entirely within this simultaneous field of view (SFOV). The thyroid 7P collimator differs from the heart 7P collimator in the following respects:

1. The diameter of the pinholes is 4 mm instead of 7 mm. This improves the resolution throughout the simultaneous field of view (SFOV) of the system, but reduces the sensitivity.

2. The distance from the collimator to the detector is 60 mm instead of 127 mm. This implies that the distance between the organ and the detector is considerably smaller as well, which has a positive effect on both the resolution and the sensitivity of the device.

The SFOV is divided into eight slices of 7.5 mm thickness beginning at 41.3 mm from the collimator midplane, i.e., 35.5 mm from the outer surface of the collimator plate (Fig. 2).

The in-plane voxel size varies from 3.1 mm × 3.1 mm in the first slice (nearest to the collimator) to 6.1 mm × 6.1 mm in the last slice. These sizes are approximately a factor of 2 smaller than the corresponding ones of the heart 7P collimator. This reflects the fact that we expect a better resolution of the present device.

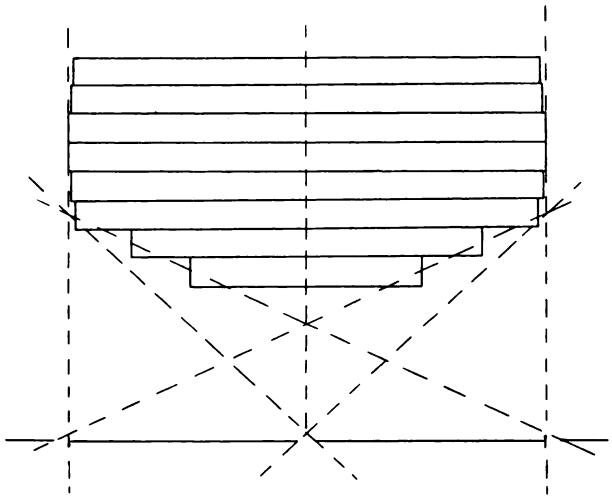

FIGURE 2
The eight reconstruction slices in the simultaneous field of view. The dashed lines are the boundaries of three projection cones (one central, two peripheral).

The camera data are digitized in a 128 × 128 pixel (picture element) frame. The number of pixels for which the count rate is used for reconstruction is 8,232 (7 × 1176), while the number of voxels (volume elements) of which the intensity is to be reconstructed is equal to 4,468.

The *time-coded aperture* was originally proposed by Koral et al. (*6*). It essentially consists of two lead plates, one of which (the code plate) contains a pattern of pinholes, the other (the aperture plate) contains a large square opening defining an 11 × 11 pinhole area (Fig. 3). Using electric stepping motors, the code plate is shifted over the aperture plate such that for each plate position a different pattern of pinholes lies in front of the square opening. Data are collected in 121 time intervals (or plate positions), during each of which there are always exactly 40 pinholes in front of the aperture. On the one hand, this means that the sensitivity of the device is high. On the other hand, however, the acquisition time for each plate position is short, so relatively few counts reach the detector in one time interval. Furthermore, there will be 40 overlapping pinhole projections of the thyroid on the crystal.

The data acquisition time interval is equal for each plate position and is set prior to the data collection process to a value in between 8 and 13 sec (the total acquisition time will then lie in between 19 and 29 min). Smaller time intervals would yield statistically unacceptable data; larger time intervals are considered unacceptable for the patient.

The electronics for the motors and for the specific movement of the code plate are built into a separate device controller console that also contains the hardware needed for communication with the host computer.

Some *system parameters* follow below. The camera data are digitized into a 64 × 64 pixel frame. The distance from the midplane of the code plate to the detector is 145 mm. The spacing between the centers of adjacent pinholes is 5 mm and the dimension of the pixels is also chosen to be 5 mm × 5 mm. The diameter of the pinholes is equal to 3.2 mm. The object space is divided into eight slices of 7.5 mm thickness all lying parallel to the collimator (the reconstruction volume starts at 26.3 mm from the midplane of the code plate). Only a very small part of the reconstruction volume can be 'seen' through all pinhole positions. The simultaneous field of view is far too small to encompass the complete thyroid and, therefore, the whole field of view should be reconstructed (this differs from the situation in the 7P case). The total number of raw data (pixel count rates) is 256,036, while the number of voxels from which the intensity is to be reconstructed is

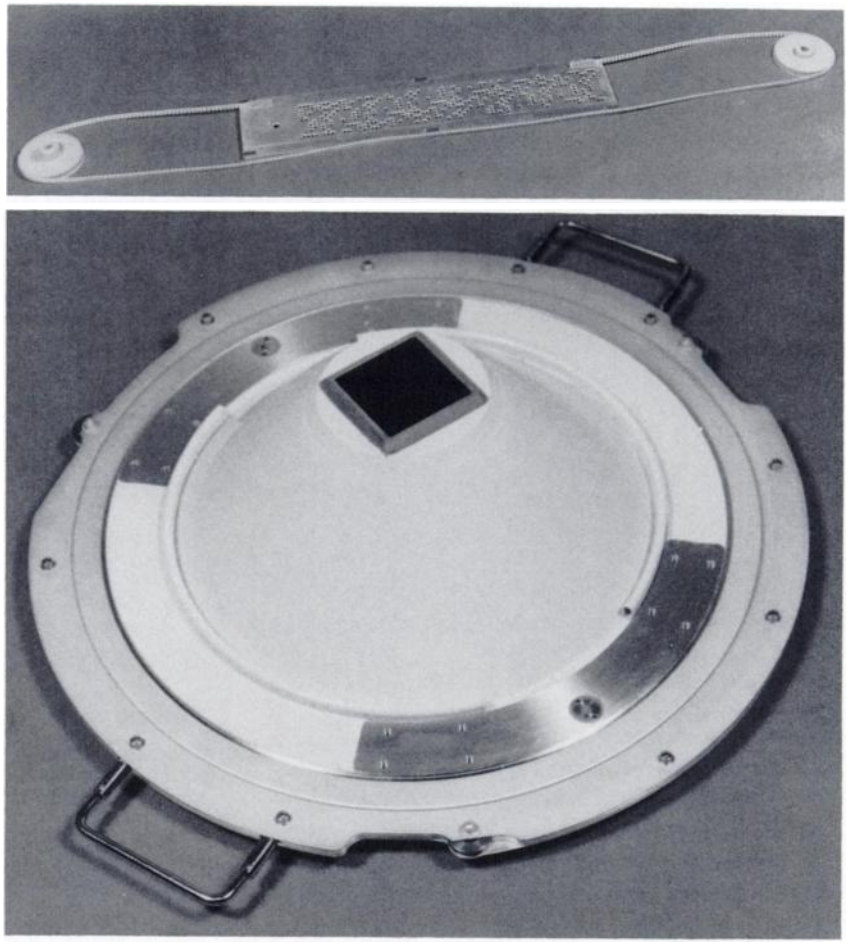

FIGURE 3
The code plate with its pattern of pinholes (top). Note that the plate also contains a larger pinhole for patient positioning. The aperture plate (bottom) consists of a flat circular lead disk with a large square opening defining a 11 × 11 pinhole area.

59,980. The in-plane voxel dimensions vary from 1.0 × 1.0 mm^2 in the slice nearest to the collimator to 2.8 × 2.8 mm^2 in the slice farthest away.

The data acquisition is performed with a smaller dedicated computer system that is attached to the gamma camera and that also communicates with the TCA controller. The raw data frames are stored on a dual-ported 300 Mbyte disk of which the second port is connected to the main computer on which the reconstruction is performed.

Preprocessing and Reconstruction

For both the 7P collimator and the TCA system, the raw projection data have to be preprocessed in order to correct for improper gamma camera settings.

For the 7P collimator the following procedure is followed.

1. The 7P projection of a reference point source is used to spatially transform raw projection data such that these will fit the configuration expected by the reconstruction software.

2. The image of a sheet source is used to correct for system geometry (i.e., to make the projection data invariant to the angle of incidence of the rays on the detector). This correction simultaneously compensates for gamma camera inhomogeneities (which is not particularly necessary because of the correction electronics in the gamma camera head).

For the TCA device the preprocessing step is more complicated.

1. First, each raw 64 × 64 frame is transformed so that all pixels have a physical dimension of 5 mm in both the x- and the y-direction. Second, we correct for x- and y-offsets in the gamma camera electronics, by shifting each 5 mm × 5 mm pixel frame so that its geometric center lies on the axis of the system. The values of the scale factors and the offsets are extracted from the projection of an on-axis point source located at a specific distance from the aperture. Given the geometry of the system, we can calculate exactly where we should find the 40 projections of the point source on the detector. The scale factors and the offsets can then be determined from the measured positions by using a least squares optimization algorithm.

2. Once a 64 × 64 frame is properly scaled and translated, we extract a 46 × 46 pixel frame from its center. The 46 × 46 pixel frames are used as input for the decoding process.

3. The multiplexing of the 40 thyroid projections on the crystal surface entails that each pixel will register counts coming from different parts of the object. A proper reconstruction is possible only when one knows for each pixel how many counts come from which direction. Therefore, the projection data have to be decoded before reconstruction can take place. How the decoding of the data is performed is discussed in detail elsewhere (*2,6,7*). The result of the decoding process is a set of 121 46 × 46 frames, each belonging to one pinhole position in the aperture as if only that pinhole was open during acquisition. This implies that after decoding we have 121 single pinhole projections of the thyroid. These single

pinhole projections can be corrected for system geometry. This correction, performed using the mathematically calculated projection of a sheet source through the corresponding pinhole, will compensate for the different angles of incidence of the radiation falling through the pinhole upon the detector. Note that such a mathematic correction will not compensate for detector nonlinearities and nonuniformities. In the present situation, we assume that this is taken care of by the correction electronics in the gamma camera head. We should also note that the demultiplexing of the data induces noise, that is partly, but not completely, suppressed by the reconstruction procedure. Finally, it is important to note that the decoding process can be performed during data acquisition by determining the scale factors and offsets for the preprocessing before the acquisition process is started.

The image reconstruction problem can be translated into a set of linear equations for both devices. In order to solve these two matrix equations, we use a variant of an algebraic reconstruction technique (ART3) that was proposed by Herman (*10*). A discussion of our algorithm can be found in an earlier paper (*5*).

After reconstruction, the reconstructed TCA slices are processed with a filter we called FIZEVO (FInd ZEro VOxels). This operator resets the intensity of all nonzero voxels to zero if they contribute to a zero-valued pixel† surrounded by zero-valued neighbors. We also examined the effects of this operator (and several variants of it) on the 7P reconstructions, but found that the quality of the reconstructions was not significantly improved.

Phantom Experiments

We performed the following phantom experiments in order to assess the applicability of both devices.

Point source resolution studies. In order to determine point source FWHM resolution of the system throughout the reconstruction volume, we have acquired data with a small cobalt-57 emitter (diameter 0.4 mm). By fitting the reconstructed point sources with three-dimensional gaussoids we obtain the FWHM point source resolutions.

Thyroid phantom studies. We used the Picker thyroid phantom in our experiments. It contains three cold spots of 6, 9, and 12 mm diameter, respectively, and one (local) hot spot of 12 mm diameter. The phantom is filled with a technetium-99m solution, and is placed within the field of view such that its midplane coincides with the boundary surface between slices 4 and 5.

Patient Studies

All patients were administered a dose of 30 MBq iodine-123 (^{123}I) intravenously, 4–5 hr prior to the data collection. First the 7P data are collected (that takes 10–30 min depending on the count rate: the acquisition is stopped if 750k counts have been collected or if the maximum acquisition time of 30 min is exceeded), followed by the TCA data. The acquisition time interval for the TCA data collection is normally set such that the total acquisition time is equal to 19 min. For those cases where the count rate is very low, this time interval can be adjusted. In between the two data collection sessions a break of half an hour is inserted so as to give the patient some rest, to replace the 7P collimator by the TCA, and to readjust the settings of the gamma camera. A few patients were also subjected to the conventional method of thyroid imaging using a single pinhole collimator. In this technique, three images are acquired from different angles (anterior, left anterior oblique, and right anterior oblique), which is why this method is sometimes called multiple view pinhole imaging (MVPI). For the patients in question the results of MVPI will be included in the discussion.

RESULTS

Table 1 presents the results of FWHM studies for the 7P collimator. The average of the in-plane resolution fxy is 4.9 mm with a standard deviation of 0.3 mm. The z resolution fz averages 5.6 mm (s.d. = 0.8 mm). Hence, in-plane resolution and depth resolution are almost equal. Moreover, the figures indicate that, as expected, fxy and fz are correlated with the distance from the point source to the collimator: the nearer to the aperture plate, the better the resolution.

The poor depth resolution for extended sources is one of the greater drawbacks of incompletely sampled systems. It would, therefore, be interesting to show and discuss the in-depth point response function since this would help to understand the performance of the system in the case of an extended source. However, the severe undersampling of the object volume in the z-direction (7.5 mm slices) precludes the possibility of a reliable calculation of the in-depth point response function. This reasoning also applies to the TCA device of which Table 2 shows the FWHM resolution figures. The average in-plane (xy) resolution is 3.6 mm (s.d. = 0.4 mm) and the z resolution averages 4.8 mm (s.d. = 0.4 mm). Moreover, the data in Table 2 clearly shows that also for the TCA device the resolving power in both the xy- and the z-direction decreases with increasing distance to the aperture.

Figure 4 shows the thyroid phantom reconstructions for both devices. The 7P reconstruction is nice and smooth, whereas the TCA reconstruction contains more

TABLE 1
7P FWHM Resolution Values for Point Sources in Air (in mm)*

	r = 0		r = 10		r = 20		r = 30		r = 40	
z	fxy	fz	fxy	fz	fxy	fz	fxy	fz	fxy	fz
52.5	4.4	4.9								
60.0	4.6	4.7	4.6	4.2	4.5	4.5	4.6	4.9	4.7	5.1
67.5	4.8	5.2			4.7	5.2			4.8	5.3
75.0	5.0	5.9			4.8	5.6	4.9	5.6	4.8	5.7
82.5	5.1	6.5							5.0	6.1
90.0	5.3	7.1	5.1	6.8	5.2	6.5	5.3	6.5		

* z Distance (mm) from the point source to the pinhole plane, r distance (mm) to the detector axis, fxy FWHM resolution parallel to the detector plane, fz FWHM resolution parallel to the system axis.

TABLE 2
TCA FWHM Resolution Values for Point Sources in Air (in mm)*

	r = 0		r = 10		r = 20		r = 30		r = 40	
z	fxy	fz	fxy	fz	fxy	fz	fxy	fz	fxy	fz
37.5	3.0	4.1			3.1	4.2			3.0	4.1
45.0	3.2	4.4	3.3	4.3	3.2	4.2			3.2	4.3
52.5	3.3	4.8			3.4	4.7			3.4	4.8
60.0	3.5	4.8	3.6	4.8	3.6	5.0	3.5	5.0	3.6	4.8
67.5	3.6	5.0			3.8	5.4			3.7	5.1
75.0	3.8	5.2	3.9	5.1	4.0	5.4	3.9	5.5	4.0	5.2

* *z* Distance (mm) from the point source to the pinhole plane, *r* distance (mm) to the detector axis, *fxy* FWHM resolution parallel to the detector plane, *fz* FWHM resolution parallel to the system axis.

noise. Furthermore, the 7P device apparently has a better resolution in the direction along the axis of the system. This is understandable because the midplane of the SFOV of the 7P system is viewed from a range of 44°, whereas the corresponding viewing range for the TCA is 24°. In the 7P reconstruction two cold spots can be clearly distinguished, but the third one appears to be too small (6 mm in diameter) to be detected. In the TCA reconstruction, however, this cold spot can be observed quite well. According to these phantom experiments it is hard to tell which of the two devices is more appropriate for thyroid tomography. This decision can only be made on the basis of the patient studies which will be discussed in the next paragraph. A more extensive description of the phantom experiments can be found elsewhere (*1,2*).

We have recently begun performing patient studies in order to evaluate and compare the two devices. Four of these studies are discussed here.

Figure 5 shows a patient with a normally functioning thyroid. In the 7P reconstruction we can observe artifacts in the first few slices. The TCA reconstruction is less smooth but it seems to have a better in-plane resolution. It should be mentioned here, that during acquisition of the TCA data, the patient had great difficulty in lying motionless (she had neuritis in her right arm and had to be massaged all through the data acquisition which instigated small movements of the body and thus of the thyroid). The quality of the reconstruction indicates that the TCA system is not very sensitive to slight patient movements during acquisition. The 7P device is, of course, less sensitive still because only one picture is acquired in ~20 min.

We included Figure 6, that shows reconstructions of a patient with a very large thyroid, to point out an advantage of the TCA over the 7P collimator. The 7P reconstruction shows that the collimator was not properly positioned. This can partly be blamed on the fact that positioning must be performed with the same (4 mm diameter) pinholes as are used for the actual data collection. It can therefore take a while before enough counts have been collected to judge whether the collimator is in position, especially if the thyroid has taken up very little of the injected ^{123}I dose and/or has an unfamiliar shape (both arguments apply in the present study). In clinical routine, the time spent on positioning will be minimal, that may sometimes result in incorrect positioning. The TCA plate has a special positioning pinhole with a relatively large pinhole diameter (7 mm). This means that positioning can be done three times as fast as with the 7P collimator which implies less mistakes and more accurate positioning. The 7P recon-

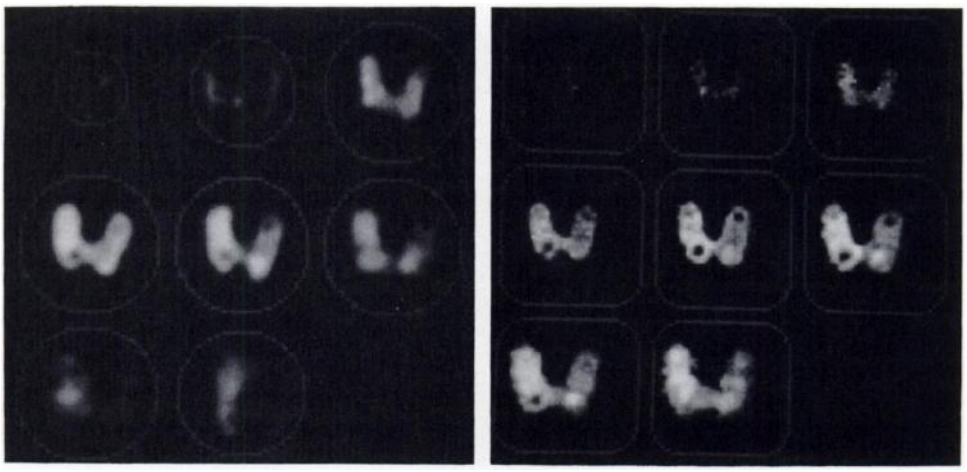

FIGURE 4
Reconstructions of the Picker thyroid phantom filled with a 5 MBq ^{99m}Tc solution. With the 7P collimator (reconstruction shown on the left) a total of 707k counts were collected in 8 min. The TCA device (reconstruction shown on the right) collected a total of 2.8*M* counts in 7 min and 40 sec. The reconstructed tomograms are stored from left to right and from top to bottom (the upper left slice is nearest to the collimator). Each of the slices is encompassed by a circle (for 7P reconstructions) or by a 'square' (for TCA reconstructions) to indicate its boundary.

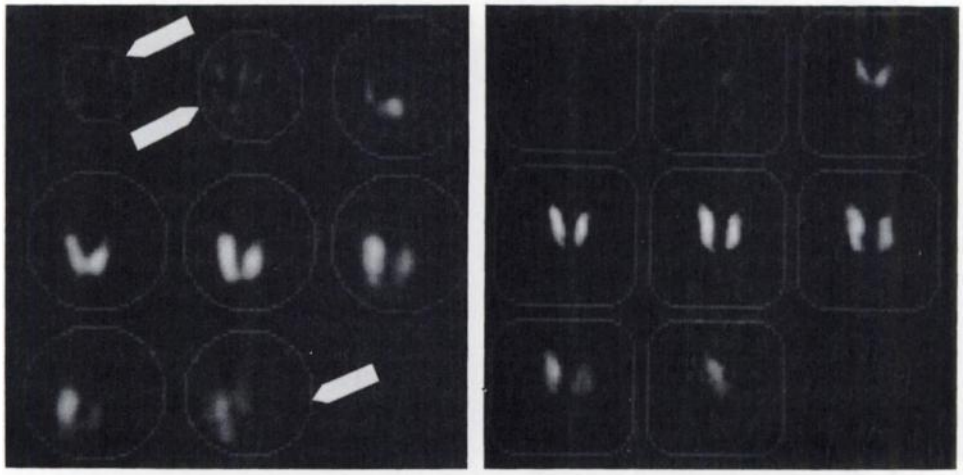

FIGURE 5
63-yr-old female patient with a normal thyroid gland. With the 7P collimator (reconstruction on the left) a total of 750k counts were collected in 12 min. The TCA device collected a total of 7.4*M* counts in 19 min. Note the artifacts in the 7P reconstruction (arrows).

struction contains a lot of artifacts in the first slices, not in the least because of incorrect positioning. The part of the thyroid that can be observed, indicates that the left lobe is very large and has accumulated almost no activity. The right lobe seems to function properly. The TCA reconstruction shows a relatively noisy picture because of the low count rate. During the total acquisition (which was, in fact, too short), 3.3*M* counts were collected which is less than the minimum 4.5*M* counts that we found were necessary for a proper reconstruction (*2*). Nonetheless, the TCA reconstruction demonstrates that the left lobe is very large and cold and that the right lobe is normal of size and activity.

Figure 7 shows a patient for which the 7P and the TCA reconstructions can be interpreted differently. The 7P reconstruction is smooth and does not contain many artifacts. On initial observation, the thyroid appears to be functioning normally. On closer inspection, however, two hot spots may be observed: in the right lobe near the top and in the left lobe near the bottom. The TCA reconstruction, though noisier, gives much more detailed information about the locations and the dimensions of the two hot spots. An accompanying MVPI study clearly demonstrates the presence of these two hot spots, but does not give any detailed information about their respective positions and sizes.

Figure 8 shows a patient with a small hot spot on the isthmus. This hot spot can be observed in the third slice

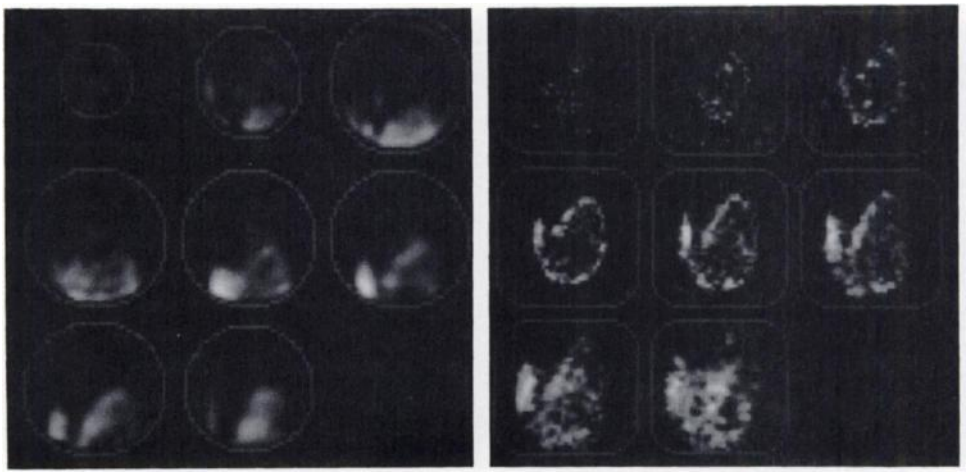

FIGURE 6
55-yr-old female patient with a large left lobe in which almost no activity has accumulated. Left: 7P reconstruction (630k counts were collected in 23 min). Right: TCA reconstruction (3.3*M* counts in 19 min). Note that the 7P collimator was positioned incorrectly.

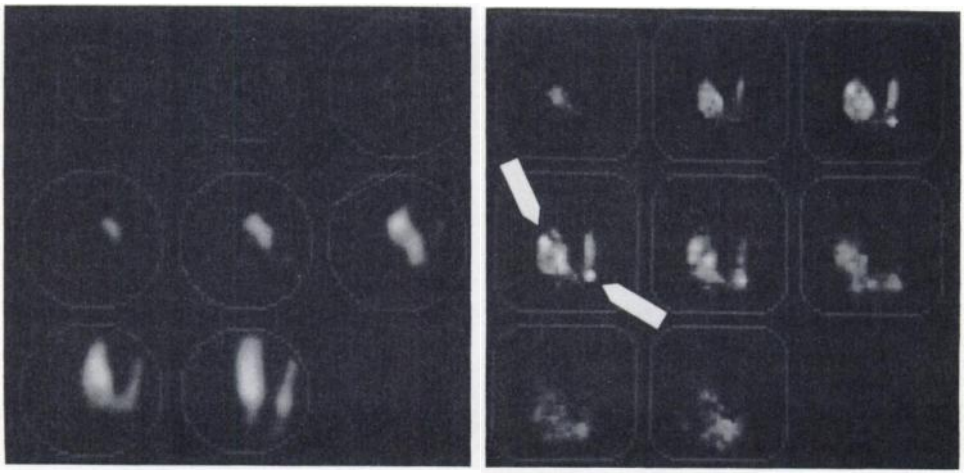

FIGURE 7
33-yr-old female patient with two hot spots in the right lobe. Left: 7P reconstruction (750k counts were collected in 20 min). Right: TCA reconstruction (6.0*M* counts in 19 min). Improved detection of the two hot spots (arrows) is demonstrated by the TCA images.

of the 7P reconstruction and in slices 2 and 3 of the TCA reconstruction. The diameter of this more or less circularly shaped spot that can be derived by measurement from the TCA tomograms, is ~4 mm. In the 7P reconstruction, the diameter of the spot is rather large and its intensity (relatively) low. Both these effects can be ascribed to the "smoothing properties" of the 7P technique. Because of the large diameter of the hot spot and its relatively low intensity on the one hand, and because of the position of the spot (on the outer surface of the isthmus nearest to the collimator) on the other hand, this defect can easily be "overseen" and interpreted as being a normal part of the thyroid (compare with Figure 5, slice 3). Furthermore, both 7P and TCA reconstructions show that the two lobes are of normal shape and size and do not contain any other abnormalities.

DISCUSSION

The anatomy of the thyroid gland and the diseases affecting it make high resolution tomographic imaging desirable. The two devices discussed in this paper both have tomographic capabilities. Another reason to investigate these techniques is that, in theory, the two devices have the following advantages over the standard thyroid imaging technique (MVPI).

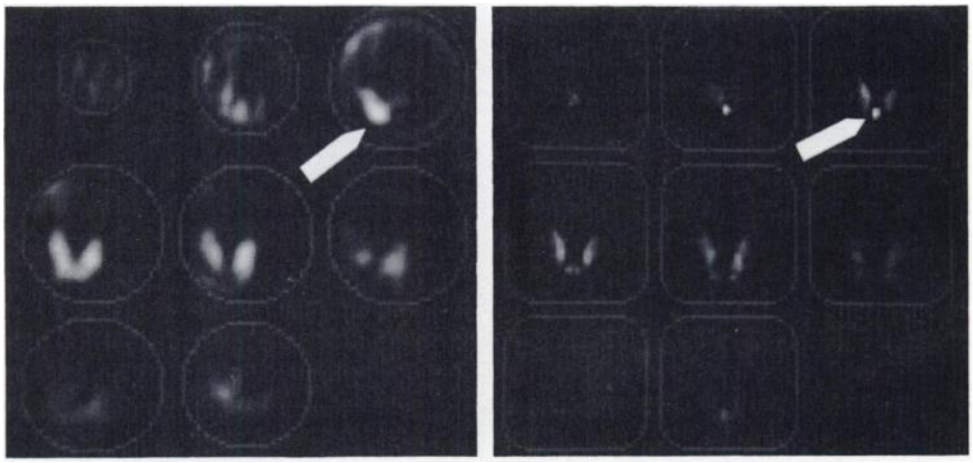

FIGURE 8
37-yr-old female patient with a hot spot on the isthmus (arrows). The 7P reconstruction (500k counts in 30 min) is shown on the left and the TCA reconstruction (2.4*M* counts in 29 min) on the right. Note that the hot spot is very clear in the TCA reconstruction, but can easily be overseen in the 7P reconstruction.

1. The size of the thyroid and the sizes of defects can be measured from the tomograms. Consequently, the volume of the thyroid and of abnormalities in the thyroid can be estimated. This can be valuable to radionuclide therapy.

2. The inherent high contrast of reconstructed tomographic images leads to improved lesion detectability (this is particularly important for cold lesions).

3. The efficiency of the devices (especially of the TCA) is quite good because they can be placed in close proximity of the thyroid. This implies that small holes can be used and, accordingly, that the resolution of the systems is high.

4. The imaging time is shorter, not in the least because repositioning is not necessary.

From the patient studies the following conclusions can be drawn.

1. From almost all studies it is obvious that positioning of the TCA device is easier than positioning of the 7P system. In order to improve positioning of the 7P system, the construction of the collimator should be modified such that is contains a larger (e.g., 7 mm) positioning pinhole. It seems worthwhile to consider the use of smaller imaging pinholes in order to improve the resolution of the device in exchange for a loss in sensitivity (resulting in less smooth images).

2. Most 7P reconstructions contain artifacts in the first few slices, whereas TCA images contain more noise. These effects can easily be explained.

During the 7P reconstruction only the activity within the SFOV is reconstructed. The 7P projection data, however, may contain contributions from areas outside the SFOV (especially in the case of incorrect positioning). The reconstruction algorithm will have problems with reconstructing this extraneous radiation because it can only attribute radiation to voxels within the SFOV. This process will induce artifacts.

The signal-to-noise ratio in an element of the reconstructed TCA image (voxel) has been shown to depend on the entire source distribution (*6*), and is, therefore, very difficult to calculate. We can only give an indication of the average noise in the reconstruction which should be a function of the average source distribution and, thus, of the average number of counts per pixel. Working on the premise that during the complete acquisition a total of $6M$ counts are collected, we find that for one data acquisition time interval (one plate position) the average number of counts per pixel is ~15, which is rather low (for the thyroid 7P collimator, the average is ~90 counts per pixel for a 750k counts study). It is not very surprising, therefore, that the reconstructions contain some noise, especially in those regions where the source intensity is low (outside the thyroid).

3. From the studies it is obvious that the 7P device does not fully meet our expectations. The reconstructions look nice and smooth, but this smoothness can be misleading because it may conceal smaller abnormalities. The TCA device, however, has very good potentialities. Even small abnormalities can be observed in the tomograms.

On the basis of the above phantom experiments and patient studies we conclude that the TCA device provides a promising method for thyroid imaging, especially because we have removed the main objection against this device: the prohibitively long reconstruction time. We expect that the method is better suited for thyroid imaging than MVPI, because it combines high resolution tomographic capabilities with other advantages such as size relationship maintainance, high efficiency, shorter imaging time and improved lesion detectability. Final conclusions will have to await a more thorough clinical evaluation.

The 7P device is able to detect abnormalities and to give information on the dimensions of the thyroid, but does not appear to produce reconstructions of a quality high enough to compete with the TCA imaging system. Further studies are mandatory in order to investigate whether our preliminary conclusions concerning the two devices hold true and to test whether the theoretical advantages of the two devices over MVPI are confirmed in a clinical setting.

NOTES

* Normally, the deterioration of the resolution with increasing distance to the collimator is taken into account by using slices with increasing thicknesses. In clinical practice, however, a nonconstant slice thickness makes quantitative evaluation of the reconstruction more difficult.

† In this context a pixel is an element of a preprocessed frame rather than an element of a raw data frame.

REFERENCES

1. van Giessen JW, Viergever MA, de Graaf CN. Seven-pinhole tomography of the thyroid. *IEEE Trans Med Imag* 1986; 5:84–90.
2. van Giessen JW, Viergever MA, de Graaf CN, et al. Time-coded aperture tomography: experimental results. *IEEE Trans Med Imag* 1986; 5:222–228.
3. Vogel RA, Kirch DL, LeFree MT, et al. A new method of multiplanar emission tomography using a seven pinhole collimator and an Anger camera. *J Nucl Med* 1978; 19:648–654.
4. LeFree MT, Vogel RA, Kirch DL, et al. Seven pinhole tomography—a technical description. *J Nucl Med* 1981; 22:849–855.
5. van Giessen JW, Viergever MA, de Graaf CN. Improved tomographic reconstruction in seven-pinhole imaging. *IEEE Trans Med Imag* 1985; 4:91–103.
6. Koral KF, Rogers WL, Knoll GF. Digital tomographic imaging with time modulated pseudo-random coded

aperture and Anger camera. *J Nucl Med* 1975; 16:402–413.
7. Koral KF, Rogers WL. Application of ART to time-coded emission tomography. *Phys Med Biol* 1979; 24:879–894.
8. Koral KF, Freitas JE, Rogers WL, et al. Thyroid scintigraphy with time-coded aperture. *J Nucl Med* 1979; 20:345–349.
9. Resinger WW, Rose EA, Keyes JW, et al. Tomographic thyroid scintigraphy: comparison with standard pinhole imaging: concise communication. *J Nucl Med* 1981; 22:638–642.
10. Herman GT. A relaxation method for reconstructing objects from noisy x-rays. *Math Progr* 1975; 8:1–19.